

Acceptor related photoluminescence from ZnO:Sb nanowires fabricated by chemical vapor deposition method

C.H. Zang^{a,b}, D.X. Zhao^{a,*}, Y. Tang^{a,b}, Z. Guo^{a,b}, J.Y. Zhang^a, D.Z. Shen^a, Y.C. Liu^c

^a Key Laboratory of Excited State Process, Changchun Institute of Optics, Fine Mechanics and Physics,
Chinese Academy of Sciences, Changchun 130033, PR China

^b Graduate School of Chinese Academy of Sciences, Beijing 100039, PR China

^c Center for Advanced Optoelectronic Functional Materials Research, Northeast Normal University, Changchun 130024, PR China

Received 22 October 2007; in final form 13 December 2007

Available online 23 December 2007

Abstract

Single-crystal Sb doped ZnO nanowires were fabricated on Si (100) substrate by a chemical vapor deposition method. The photoluminescence properties of ZnO nanowires were studied with the temperature ranging from 81 to 306 K. At 81 K, the recombination of the acceptor-bound exciton was predominant in PL spectrum, which was attributed to the transition of the $(\text{Sb}_{\text{Zn}}-2V_{\text{Zn}})$ complex bound exciton. The activation of A^0X and the acceptor binding energy had been calculated to be 16.8 and 168 meV, respectively.

© 2007 Elsevier B.V. All rights reserved.

1. Introduction

One-dimensional (1D) materials such as nanowires (NWs), nanobelts (NBs), and nanorods have attracted much attention in recent years [1,2]. Among them, 1D ZnO nanostructures materials have been paid great attention, because ZnO is with a direct wide band gap (3.37 eV) and large exciton binding energy (~ 60 meV) at room temperature, which makes ZnO nanostructures materials have a potential applications on ultra-violet (UV) nanolasers and photodetectors [3]. To realize these nanodevices, p-type ZnO NWs are essential. By now, most efforts to grow p-ZnO materials have been focused on the fabrication of ZnO thin films. Some articles have reported that N, P, As, Li are as typical dopants to obtain p-ZnO thin films, but few articles commented on the fabrication of p-ZnO nanostructures materials. In addition, the electrical measurement method is also a problem to measure the conduction type of the doped ZnO nanostructures materi-

als. To obtain an efficient p-ZnO film, Limpijumnong et al. proposed a model for large-size-mismatch group-V dopants in ZnO [4,5]. It has been predicted that Sb would occupy the Zn site and simultaneously induce two Zn vacancies to form a complex $(\text{Sb}_{\text{Zn}}-2V_{\text{Zn}})$, with a low acceptor-ionization energy of ~ 160 meV, which paved the road to research Sb dopants p-type conduction semiconductor films. Following theoretic breakthrough, ZnO:Sb films with p-type conduction have been fabricated by MBE method [5]. The fabrication of ZnO:Sb NWs have also been reported [6], however its optical properties have not been researched. In this Letter, we try to grow Sb doped ZnO NWs, then photoluminescence measurements are used to observe the acceptor related emission peaks.

2. Experiment and details

In this Letter, the NWs were prepared by a vapor-solid method on a silicon substrate. 4 N Zn powder and 5% 3 N Sb_2O_3 were used as source materials. The sample was grown at 680 °C in N_2 ambient with a rate of 50 SCCM for 1 h. Then, it was thermal processed in O_2 atmosphere at 700 °C for 5 min. The sample was investigated by

* Corresponding author. Fax: +86 431 85682964.

E-mail address: dxzhao2000@yahoo.com.cn (D.X. Zhao).

field-emission scanning electron microscopy (FESEM, Hitachi-4800), energy-dispersive X-ray spectroscopy (EDS, GENE SIS 2000 XMS 60S, EDAX, Inc.) attached to an SEM, transmission electron microscopy (TEM), and a D/max-RA X-ray spectrometer (Rigaku). Photoluminescence (PL) measurements were performed using a He–Cd laser line of 325 nm as the excitation source.

3. Results and discussion

Fig. 1a and b shows the FESEM images of as-grown sample. Some NWs with the diameter of 30–60 nm and the length of several millimeters were observed on the Si (100) substrate surface. From Fig. 1c, the EDS analysis indicates that there are only zinc, oxygen and antimony elements in the NWs with almost stoichiometric content ($\text{Zn}:\text{O} = 0.52:0.48$). And the Sb concentration in NWs is about 1%. The containing Al in the sample originates from substrate aluminum tray. SAED pattern of single NW is shown in Fig. 1d, which confirms NWs are single crystalline with ZnO wurtzite structure. The structure property of NWs was also characterized by X-ray diffraction (XRD) pattern, as shown in Fig. 2. All diffractive peaks can be indexed to hexagonal wurtzite ZnO, and no diffraction peaks from any other minerals were observed.

The UV resonant Raman scattering at room temperature was performed to investigate the vibrational properties of the Sb doped ZnO NWs, as shown in Fig. 3. The Raman peaks are located at 540, 1117 and 1698 cm^{-1} . They are assigned to $A_1(\text{LO})$ multi-phonon Raman scattering mode. As well known, for bulk ZnO the frequency at 574 cm^{-1} of 1LO phonon peak corresponds to first-order $A_1(\text{LO})$ phonon, while that at 583 cm^{-1} of 1LO phonon peak corresponds to first-order $E_1(\text{LO})$ phonon [6]. However, Fig. 3 shows the 1LO peak in the ZnO

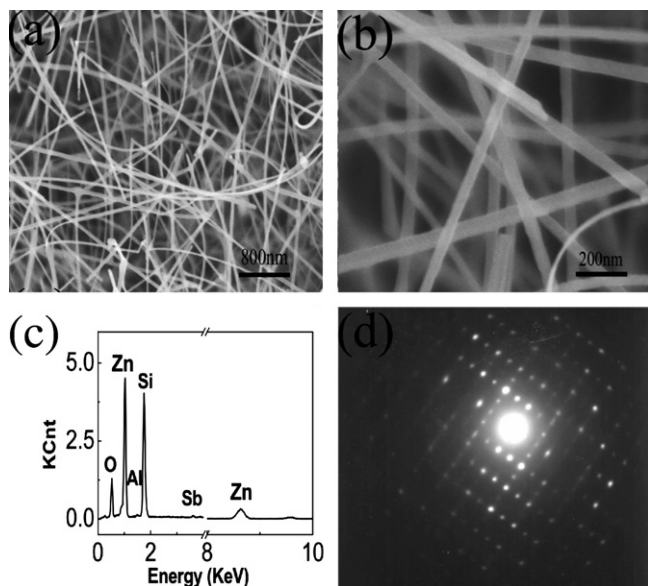


Fig. 1. The SEM images (a, b) EDX spectrum (c), and SAED images (d) of Sb doped ZnO NWs.

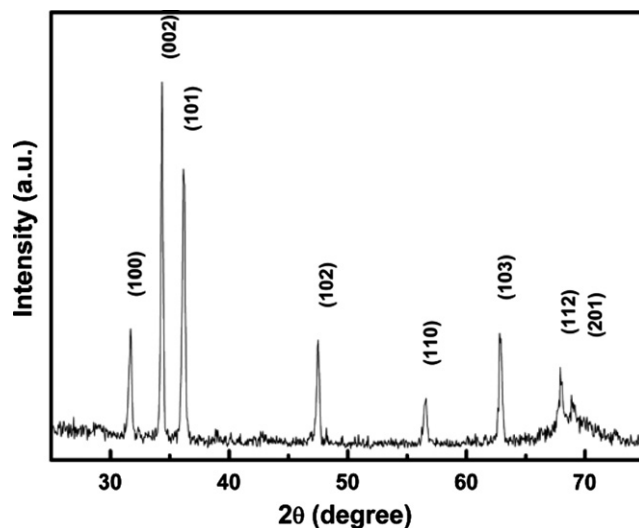


Fig. 2. The XRD pattern of Sb doped ZnO NWs.

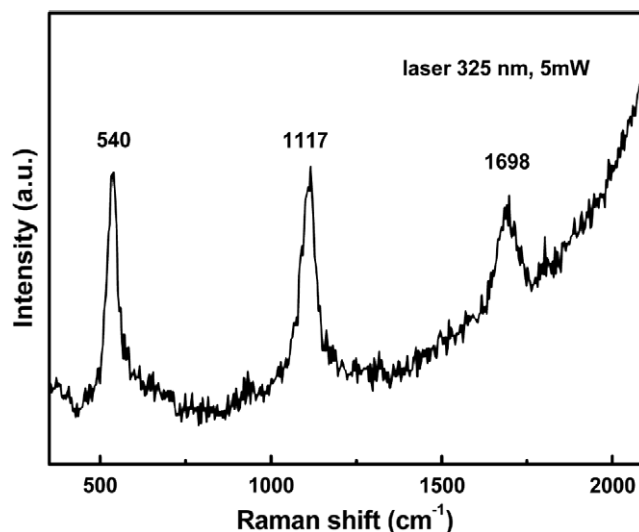


Fig. 3. The Raman spectrum of Sb doped ZnO NWs.

nanowires located at 540 cm^{-1} . The large redshift of 1LO phonon could be attributed to the local heating and the lattice deformation. The 1LO peak redshift caused by local heating could reach about 10 cm^{-1} in 20 nm ZnO QDs at 5 mW excitation power [7]. In our previous experiments, the 1LO phonon peaks in ZnO nanorods and nanowires measured at the same condition were located at 571 and 579 cm^{-1} , respectively [8]. Therefore, the effect of local heating was not predominant in our experiment. And the observed large redshift of 1LO phonon peak could be mostly attributed to the lattice deformation, which is caused by a big lattice mismatch for Sb as a dopant into ZnO lattice. The phonon peak at 531 cm^{-1} has been also observed in ZnO:Sb NWs [9].

Low-temperature PL measurements of undoped and Sb doped ZnO NWs were carried out at 81 K, as shown in Fig. 4. The PL spectrum of the undoped ZnO NWs shows

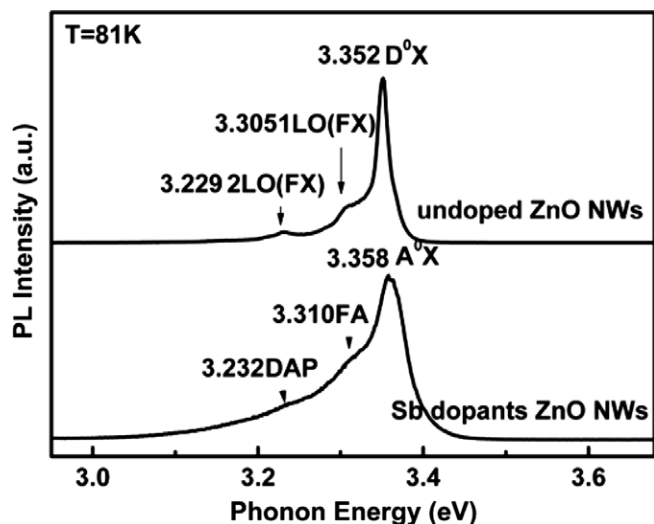


Fig. 4. The low-temperature PL spectra of undoped ZnO NWs and Sb doped ZnO NWs.

a strong near-band-edge emission located at 3.352 eV, which was assigned to the transition of neutral-donor-bound exciton (D^0X) [10]. At the high energy side of this emission peak a free exciton (FX) related emission at 3.367 eV could also be found. The emission peak at 3.305 eV is separated 62 meV from FX, which was assigned as 1LO (FX). For Sb doped ZnO NWs, the PL spectrum shows that well-resolved emissions located at 3.358, 3.310 and 3.232 eV, which could be attributed to the radiant recombination from neutral-acceptor-bound exciton (A^0X), free electron to the acceptor transition (FA) and donor-acceptor pair (DAP), respectively. The acceptor related peak position for Sb doped ZnO samples is quite different from the undoped one. The peak was seen at 3.20, 3.31 and 3.32 eV for the acceptor-bound exciton in ZnO nanocrystals (NCs), quantum dots (QDs) and bulk, respectively [11]. The redshift of acceptor-bound exciton in ZnO NCs and QDs comparing to that in ZnO bulk is attributed to the large surface-volume ratio in both types of nanoparticles and, consequently, a large number of acceptor defects near the surface. The insight of the theoretical work on surface-bound excitons in ZnO nanostructures also confirmed that there were abundant surface-related acceptors existence with ZnO nano-scale decrease [12]. But in our experiment, the diameter of Sb doped NWs was beyond 30 nm. The effect of surface defect was not predominant on the optical properties of nanowires.

To further understand these emissions, the temperature-dependence PL measurement of Sb doped ZnO NWs was made ranging from 81 to 306 K, as shown in Fig. 5a. The emission at 3.232 eV showed a small blue shifts during the temperature increase, which are typical characteristic of DAP transitions. In Fig. 5b, the integrated PL intensity of UV NBE emission was also expressed as a function of the inverse of temperature. It was observed that the intensities

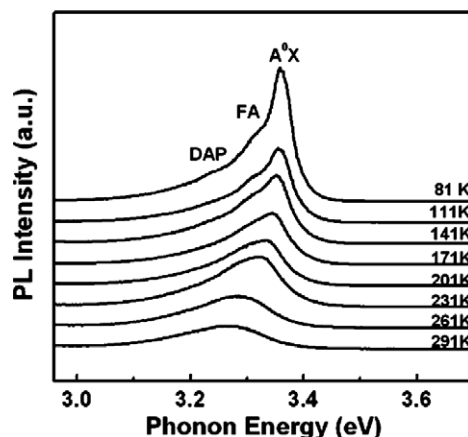


Fig. 5a. The temperature-dependence PL spectra of Sb doped ZnO NWs ranging from 81 to 306 K.

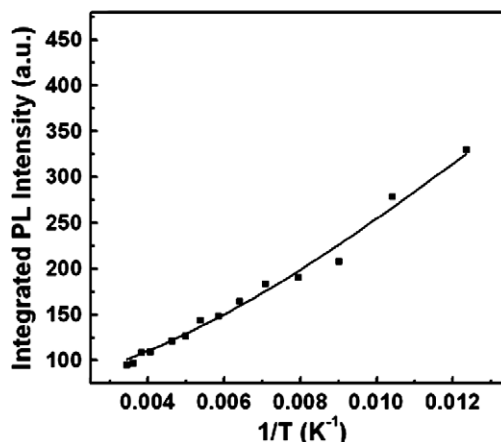


Fig. 5b. Integrated PL intensity of A^0X as a function of $1/T$ for Sb doped ZnO NWs.

decayed with the temperature T increase, in agreement with the following expression [13],

$$I = \frac{A}{1 + B \exp(-E_a/kT)}, \quad (1)$$

where A and B are scaling factors, E_a is active energy, and k is Boltzmann's constant. From Eq. (1) it can be deduced that the PL integrated intensity, I , should exhibit an exponential dependence on $1/T$. As shown in Fig. 5b, the PL integrated intensity of A^0X (filled square) was fitted according to Eq. (1), then $E_a^{A^0X} = 16.8$ meV was obtained. Using the Haynes rule $E_a^{A^0X}/E_A = 0.1$ for ZnO material system, [14], an acceptor binding energy E_A is estimated to be 168 meV. The binding energy of the acceptor E_A can be calculated with the equation

$$E_A = E_{\text{gap}} - E_D - E_{\text{DAP}} + \frac{e^2}{4\pi\epsilon\epsilon_0 r}. \quad (2)$$

The donor binding energy E_D is reported to be 60 meV [15], and the intrinsic band gap $E_{\text{gap}} = 3.437$ eV at 4.2 K [16–18], r is the separation, ϵ is the dielectric constant of

ZnO (8.6). The last term of Eq. (2) is ~ 30 – 60 meV [19]. In our experiment, the value of E_A was calculated to be 175–205 meV, which is similar to the value estimated by A^0X emission peak. The emission at 3.310 eV is assigned FA. It is well known that the majority of p-type ZnO films doped by group-V elements have an E_{FA} emission at ~ 3.310 eV [16,17,19–21]. The E_A can be calculated from the equation

$$E_A = E_{\text{gap}} - E_{FA} + K_B T / 2, \quad (3)$$

using $E_X = 3.377$ eV and $E_{cA} = 3.310$ eV at 81 K. The acceptor binding energy was calculated to be 130 meV, it is smaller than that calculated from optical active energy. The acceptor energy ~ 168 meV is attributed to Sb substituting Zn and inducing two Zn vacancies, further forming the $Sb_{Zn}-2V_{Zn}$ complex, a shallow acceptor about 160–220 meV in early report [4].

4. Conclusion

In summary, Sb doped ZnO nanowires were fabricated by chemical vapor deposition method. The XRD pattern showed ZnO with a hexagonal wurtzite structure. In the Raman spectrum, the considerable redshift of the 1LO phonon peak was mostly attributed to the surface defects and crystalline boundaries caused by the big lattice mismatch from Sb doped in ZnO lattices. The PL properties of Sb doped ZnO NWs were characterized by low temperature and temperature-dependence PL spectra. The PL spectra at 81 K, the peaks position and linewidth of the Sb doped ZnO NWs were obviously different to those of undoped ZnO NWs. And the UV emission located at 3.358 eV (81 K) was considered to be the transition of neutral-acceptor-bound exciton, which was depicted as $Sb_{Zn}-2V_{Zn}$ complex acceptor and its binding energy was calculated to be 168 meV with the help of the temperature-dependence PL spectra. This value was in good agreement with the estimated value 175–205 meV calculated from the DAP. The PL was predominant original from the acceptor-bound exciton formed inside ZnO:Sb NWs than at the surface.

Acknowledgments

This work is supported by the Key Project of National Natural Science Foundation of China under Grant Nos. 60336020 and 50532050, the ‘973’ program under Grant No. 2006CB604906, the CAS Innovation Program, the National Natural Science Foundation of China under Grant Nos. 60429403, 60506014, 50402016, 60676059 and 10674133.

References

- [1] Liang-Wen Ji, Sheng-Joue Young, Te-Hua Fang, Chien-Hung Liu, Appl. Phys. Lett. 90 (2007) 033109.
- [2] F. Fang et al., Nanotechnology 18 (2007) 235604.
- [3] Lei Luo, Brian D. Sosnowchik, Liwei Lin, Appl. Phys. Lett. 90 (2007) 093101.
- [4] S. Limpijumnong, S.B. Zhang, Su-Huai Wei, C.H. Park, Phys. Rev. Lett. 92 (2004) 155504.
- [5] J.L. Liu, F.X. Xiu, L.J. Mandalapu, Z. Yang, Proc. SPIE 6122 (2006) 61220H.
- [6] K.A. Alim, V.A. Fonoberov, Alexander A. Balandin, Appl. Phys. Lett. 86 (2005) 053103.
- [7] K.A. Alim, V.A. Fonoberov, M. Shamsa, A.A. Balandin, J. Appl. Phys. 97 (2005) 124313.
- [8] (a) X.Q. Meng, D.X. Zhao, D.Z. Shen, J.Y. Zhang, B.H. Li, X.H. Wang, X.W. Fan, J. Lumin. 122–123 (2007) 766;
(b) X.Q. Meng et al., Solid State Commun. 135 (2005) 179.
- [9] C. Bundesmann et al., Appl. Phys. Lett. 83 (2003) 1974.
- [10] F.X. Xiu, Z. Yang, L.J. Mandalapu, D.T. Zhao, J.L. Liu, Appl. Phys. Lett. 87 (2005) 252102.
- [11] V.A. Fonoberov, K.A. Alim, A.A. Balandin, F. Xiu, J. Liu, Phys. Rev. B 73 (2006) 165317.
- [12] V.A. Fonoberov, A.A. Balandin, Appl. Phys. Lett. 85 (2004) 5971.
- [13] D.S. Jiang, H. Jung, K. Ploog, J. Appl. Phys. 64 (1988) 1371.
- [14] D.C. Look, G.M. Renlund, R.H. Burgener II, J.R. Sizelove, Appl. Phys. Lett. 85 (2004) 5269.
- [15] D.C. Reynolds, D.C. Look, B. Jogai, C.W. Litton, T.C. Collins, W. Harsch, G. Cantwell, Phys. Rev. B 57 (1998) 12151.
- [16] D.K. Hwang et al., Appl. Phys. Lett. 86 (2005) 151917.
- [17] Y.R. Ryu, T.S. Lee, H.W. White, Appl. Phys. Lett. 83 (2003) 87.
- [18] L.J. Wang, N.C. Giles, J. Appl. Phys. 94 (2003) 973.
- [19] F.X. Xiu, Z. Yang, L.J. Mandalapu, D.T. Zhao, J.L. Liu, W.P. Beyermann, Appl. Phys. Lett. 87 (2005) 152101.
- [20] D.C. Look, D.C. Reynolds, C.W. Litton, R.L. Jones, D.B. Eason, G. Cantwell, Appl. Phys. Lett. 81 (2002) 1830.
- [21] T.S. Jeong, M.S. Han, C.J. Youn, Y.S. Park, J. Appl. Phys. 96 (2004) 175.